ELSEVIER

International Journal of Mass Spectrometry 185/186/187 (1999) 847–857

International Journal of Mass Spectrometry

Molecular dynamics study of the collision-induced dissociation of the methyl nitrite cation

Runzhi Zhao[1], Anil K. Shukla, Jean H. Futrell*

Department of Chemistry and Biochemistry, University of Delaware, Newark, DE 19716, USA

Received 27 July 1998; accepted 12 October 1998

Abstract

The crossed molecular beam method was used to measure scattering dynamics of the collision-induced dissociation of the methyl nitrite cation to form NO^+ plus methoxy radical at center-of-mass collision energies of 3.1, 19.8, and 39.8 eV. The collisional activation mechanism is impulsive at all these energies, with most probable scattering angles of 23°, 8°, and 5°, respectively. The average conversion of translational energy into internal energy is modest, about 0.6 ± 0.5 eV and is comparable to the thermochemical threshold for this process. The distribution of kinetic energies in the product ion is quite large and increases with increasing collision energy. Rice–Ramsperger–Kassel–Marcus calculations of the rates of dissociation of the molecular ion were used to describe the dissociation of the molecular ion as a function of internal energy. Convolution of the breakdown graph, an energy distribution based upon Massey's adiabatic criterion and kinetic energy release in the dissociation step satisfactorily rationalizes our experimental results. These results are combined with those from an earlier dynamics study of nitromethane cation to provide a general description of the role of isomerization in collision-induced dissociation occurring on their common potential energy surface. (Int J Mass Spectrom 185/186/187 (1999) 847–857) © 1999 Elsevier Science B.V.

Keywords: Collision-induced dissociation; Ion activation; Reaction dynamics; Scattering; Rate constant; Energy deposition

1. Introduction

The unimolecular dissociation of the methyl nitrite cation and its isomer, the nitromethane cation, and their interconversion have been a focus of continuing research in ion chemistry [1–15]. It has been suggested that the unimolecular dissociation of nitromethane cation involves rearrangement to the methyl nitrite structure prior to dissociation [1–6]. A previous report from this laboratory [6,7] invoked isomerization to methyl nitrite cation as the low energy pathway accessed in the collision-induced dissociation (CID) reaction dynamics of the nitromethane cation. The slow dissociation rates observed for the methyl nitrite cation to its lowest energy dissociation products have been rationalized by invoking either isomerization prior to dissociation or formation of excited electronic states [7,8,13].

Fig. 1 summarizes the energetics for the isometric structures and transition states connecting methyl nitrite and nitromethane cations to their reaction products. This diagram shows that the isomerization

* Corresponding author.

[1] Present address: Rhone-Poulenc Rorer, Collegeville, PA 19426.

In honor of Professor Mike Bowers' numerous contributions in the field of mass spectrometry and ion–molecule reactions on the occasion of his 60th birthday.

PII S1387-3806(98)14216-1

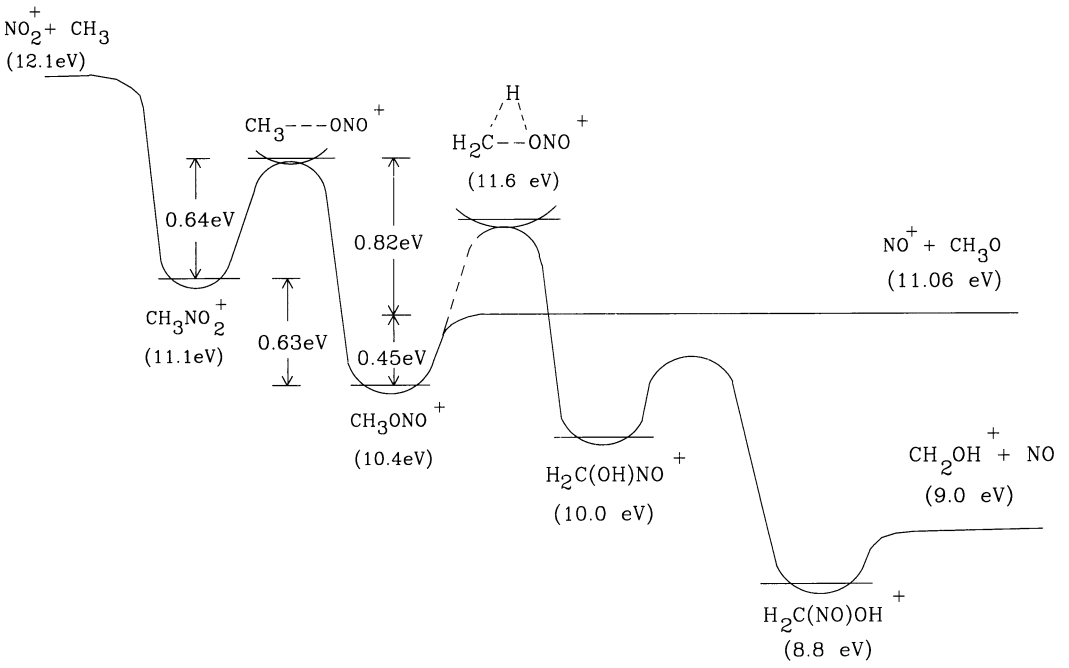

Fig. 1. Schematic potential energy diagram for the dissociation of methyl nitrite and nitromethane cations.

from nitromethane ion to methyl nitrite ion involves an energy barrier of about 0.64 eV. The present study of the CID dynamics of methyl nitrite cation decomposition represents entering the Fig. 1 surface in the potential well which has the methyl nitrite structure. We anticipate that the dynamics of this dissociation process will provide information which will both test our earlier hypothesis and provide insights into the role isomerization plays in CID processes.

The dominant unimolecular (metastable) dissociation product in methyl nitrite is the m/z 31 ion generally thought to have the CH_2OH^+ structure. A recent combined theoretical and experimental study which was concerned primarily with the CH_2OH^+ channel and the competing H-atom loss process by Schroder et al. [13] invoked hidden H-atom migrations and the formation of ion–dipole complexes as salient features of the dissociation mechanism. Although a combination of ab initio quantum chemical calculations with Rice–Ramsperger–Kassel–Marcus (RRKM) modeling reproduced details of a high resolution synchrotron radiation photoelectron photoion coincidence (PEPICO) study of deuterium isotope effect, details of this theoretical discussion has been criticized by Lorquet and co-workers [15] as incorrectly correlating the postulated CH_2OH—NO^+ distonic structure with both CH_2OH^+ (+NO) and NO^+ (+CH_2OH) asymptotes. These structures, which differ by the location of charge, are actually connected by a conical intersection avoided crossing.

The alternative description favored by Lorquet and co-workers [15] is a nonadiabatic curve-crossing mechanism to interpret the anomalous rates of formations of NO^+ and CH_2OH^+. The methyl nitrite ion either follows a diabatic potential curve to the higher asymptote leading to NO^+ or crosses to a nearly horizontal nonadiabatic curve to the lower asymptote leading to CH_2OH^+. Because the probability for following the diabatic curve is much higher than the probability for curve crossing, the low energy path is followed only when the ion has enough energy for curve crossing but not enough for dissociation to NO^+. These workers further conclude that hydrogen atom tunneling is involved in the curve crossing in

order to explain a strong isotope effect. The hypothesis that the low energy curve-crossing mechanism path is not followed in the CID of methyl nitrite cations is an attractive rationale for the present experimental results.

2. Experimental

The methyl nitrite molecule is very unstable and rapidly oxidizes when exposed to light and air. It slowly undergoes chain reaction decomposition at room temperature even when it is kept in an evacuated amber flask [16]. For this reason, methyl nitrite was synthesized and purified as needed according to a published method [17]. Briefly, concentrated sulfuric acid was slowly titrated into the mixture of sodium nitrite and methanol solution in deionized water (molar ratio of 1:1) in a closed, three-way reactor. Methyl nitrite gas thus generated was purified by passing it through calcium chloride and sodium hydroxide traps. The gas was then condensed in a stainless steel cylinder using a mixture of dry ice and acetone. Purified liquid methyl nitrite was stored at room temperature. It was checked for purity by mass spectrometry and demonstrated to have a storage life of about two months at room temperature in a stainless cylinder.

Methyl nitrite cations were generated by 70 eV electron ionization, accelerated to 3 keV for energy and mass analysis by a double focusing mass spectrometer (VG-7070) which served as the ion gun in our crossed-beam apparatus described in detail elsewhere [18]. Methyl nitrite ions were decelerated to the desired laboratory energy by a series of ion-optical lenses and focused at the collision center where it collided with a vertically moving supersonic molecular beam of helium or argon. The supersonic molecular beam was generated by expanding neat argon or helium through a 100 μm diameter capillary nozzle and passing the central core through a 1 mm diameter skimmer and a collimating chamber before colliding with the ion beam. The neutral beam is chopped by a tuning fork chopper in the collimating chamber to allow for signal averaging and subtracting the metastable and background CID contributions to the total measured signal. Fragment ions were accelerated to 100 eV by a linear-field lens for energy analysis by a hemispherical energy analyzer, mass selected by a quadrupole mass filter and detected by a Channeltron® electron multiplier (Galileo, Sturbridge, MA; model No. 4870E) operated in pulse counting mode, at a series of laboratory scattering angles by rotating the detector assembly with respect to the collision center.

Measured energy distributions were converted into velocity distributions and after necessary Jacobian transformations were plotted as a function of laboratory scattering angle. The points of equal intensity were joined together to give continuous velocity contour plots. A Newton diagram giving the velocity vectors of the ion and neutral colliders was superimposed on this plot. Since scattering is symmetric with respect to the relative velocity vector, a mirror image of these contours was drawn (as dashed lines) to show a complete picture of the scattering process. The ion and neutral laboratory velocity vectors were then removed for clarity leaving only the relative velocity vector which is finally used for estimating the energy transfer and dynamics of the dissociation process.

3. Results

NO^+ was the only ion detected with sufficient intensity that we could determine its reaction dynamics with acceptable accuracy. A strong metastable dissociation peak at m/z 31 [CH_3O^+ and/or CH_2OH^+] precluded meaningful analysis of the low intensity formation of this ion as a CID reaction product. It will be shown later that this result is entirely consistent with both recent theoretical and experimental studies of the methyl nitrite cation. No CID or metastable decay to NO_2^+ was detected in our study. The high energy barrier for the formation of NO_2^+ relative to the direct fragmentation channel to form NO^+ precludes its formation at an observable rate.

Figures 2–4 are the center-of-mass (CM) Cartesian velocity contour diagrams displaying our experimental findings for the dissociative scattering of methyl nitrite cations by collision with He or Ar at relative

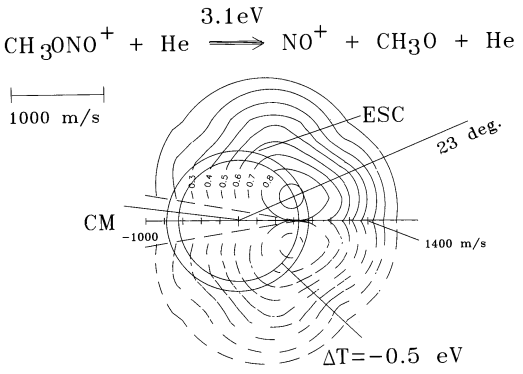

Fig. 2. CM velocity contour plot for the CID of methyl nitrite cation to NO^+ on collision with He at 3.1 eV collision energy. CM and ESC denote center-of-mass and elastic scattering circle for two-body collisions, respectively. The numbers on contours represent relative intensities of each contour. The mirror image of the plot with respect to the relative velocity vector has been drawn to show that scattering is symmetric to it. The circle marked $\Delta T = -0.5$ eV represents the most probable energy transfer from translational into internal modes in the collisional activation step.

collision energies of 3.1, 19.8, and 39.8 eV, respectively. The numbers on the contour lines in these figures designate the relative intensities of NO^+. The cone at angles drawn through the center of the highest intensity contours shows the cone of maximum intensity of the fragment ion. As explained in previous review articles [19,20] the elastic scattering circle (ESC in the figures) is the reference for estimating energy transfer in CID processes. In this analysis, we tacitly assume that CID of polyatomic ions involves a

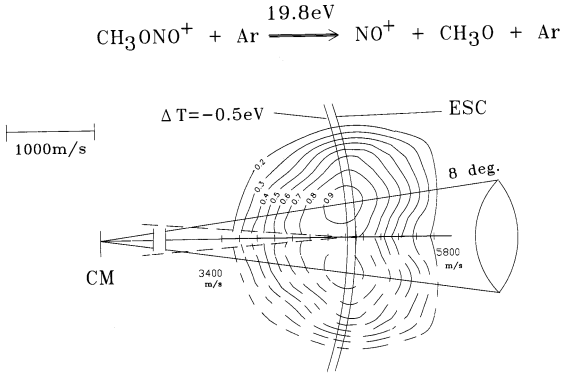

Fig. 3. CM velocity contour plot for the CID of methyl nitrite cation to NO^+ on collision with Ar at 19.8 eV collision energy.

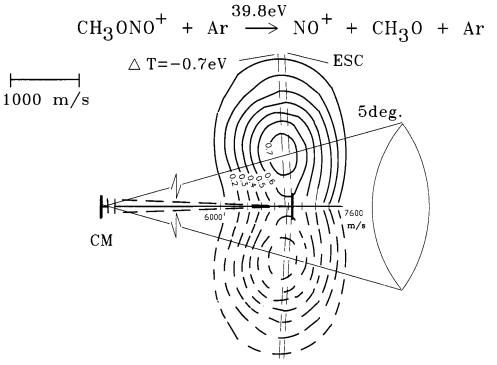

Fig. 4. CM velocity contour plot for the CID of methyl nitrite cation to NO^+ on collision with Ar at 39.8 eV collision energy.

time delay between the fast collisional excitation step (collision times typically ranging from 2 to 10 ps) and the slow dissociation step (lifetimes from picoseconds to 3 μs sampled in the present experiments).

From Figs. 2–4 we may describe the CID of methyl nitrite cation at a collision energy of 3.1 eV as exhibiting a most probable scattering angle of about 23° in the CM collision frame and a most probable energy deposition of 0.5 eV. At this energy the distribution is quite broad, with a significant distribution of fast NO^+ ions scattered outside the ESC and a significant distribution of slow particles moving with velocities only slightly greater than the CM velocity of the reactant ion and neutral. At the higher collision energies of 19.8 and 39.8 eV the dynamical mechanism remains the same. The most probable energy transfer is nearly the same (0.5 and 0.7 eV) and the most probable scattering angle closes, as expected, to 8° and 5°, respectively, at these relatively high collision energies.

The relatively large scattering angles and their energy dependence demonstrate that the dissociation is activated by impulsive collisions. The decreasing scattering angle with increasing collision energy is qualitatively consistent with a line-of-centers hard sphere collision model [21]. Similar dynamics is exhibited by propane molecular ion [22]. Scattered product ion intensity outside the ESC results either from kinetic energy release in the dissociation step or from translationally exoergic energy transfer in the

collisional excitation step. Differentiation between these possibilities requires further analysis of the experimental velocity distributions.

As described elsewhere [19,20], these Newton scattering diagrams provide valuable insights into reaction mechanisms but present a misleading picture of relative intensities and energy deposition. Proper analysis of energetics is obtained by computing the kinetic energy distribution P(T) by integrating over velocity and scattering angle, by using the relationship [23]

$$P(T) \propto U \int P_c(u_1, u_2, u_3) \sin \chi d\chi \quad (1)$$

where U is the magnitude of the product velocity relative to the CM, χ is the scattering angle in the CM frame and $P_c(u_1, u_2, u_3)$ is the probability of finding the velocity of the product ion with components u_1, u_2, u_3 in the CM Cartesian coordinate frame. P(T) diagrams are plotted by subtracting the average kinetic energy of the reactants from the P(T) distributions of products to give the relative translational energy distributions of fragment ions. These plots are called energy deposition functions.

P(T) diagrams at the three collision energies investigated are shown in Figs. 5–7. The analysis of Figs. 5–7 P(T) diagrams shows that the most probable energy transfer corresponds to 0.6 ± 0.5 eV at all three collision energies. These values deduced from Figs. 5–7 are marked as circles within the ESC in Figs. 2–4, respectively, as indices of most probable energy transfer.

The observation of metastable decay of the reactant ion into its lowest energy decomposition channel, combined with Fig. 1 energetics profile for the potential energy surface, establishes the maximum internal energy of our reagent ions to be 0.48 eV. We may therefore describe our reactant ions as having internal energies of 0.24 ± 0.24 eV. The measured most probable energy transfer increases this energy content to 0.74 ± 0.24 eV, just above the barrier height of 0.45 eV shown in Fig. 1 for the direct dissociation from methyl nitrite cation to NO^+.

The P(T) diagrams with peak widths [full width at half maximum (FWHM)] of 2.7, 7.9, and 10.5 eV

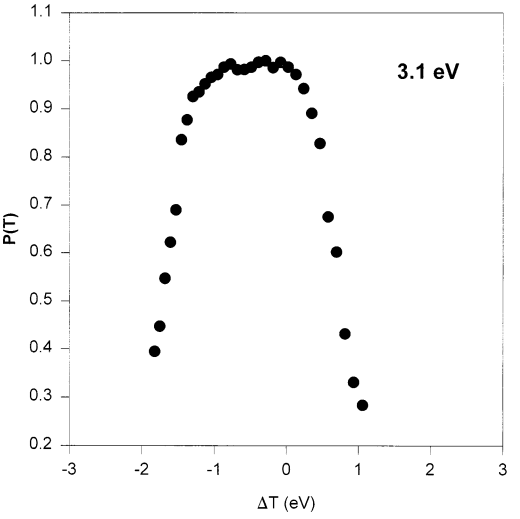

Fig. 5. Translational to internal energy transfer probability distribution for the CID of methyl nitrite cation to NO^+ on collision with He at 3.1 eV collision energy determined using Eq. (1).

further characterize CID processes at 3.1, 19.8, and 39.8 eV collision energies, respectively. These large values are the convolution of the energy deposition function with recoil kinetic energy release between the product ion and neutral in the dissociation step. As discussed previously [19,20], the latter factor is un-

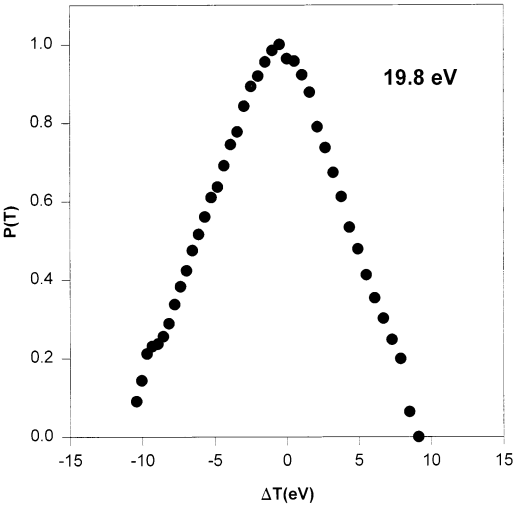

Fig. 6. Translational to internal energy transfer probability distribution for the CID of methyl nitrite cation to NO^+ on collision with Ar at 19.8 eV collision energy.

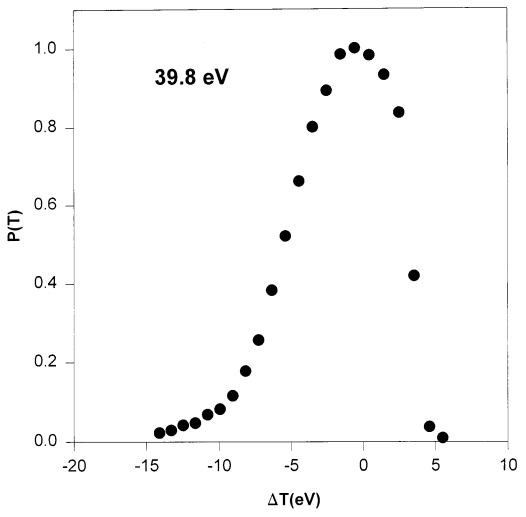

Fig. 7. Translational to internal energy transfer probability distribution for the CID of methyl nitrite cation to NO^+ on collision with Ar at 39.8 eV collision energy.

doubtedly responsible for a significant amount of the broadening of product ion velocity distributions.

There are, in fact, two CM transformations which are important in the interpretation of CID dynamics using the two-step model which we consider appropriate to the present example. The first has already been discussed in connection with the Figs. 2–4 Newton diagrams that are constructed from the momentum vectors of the reactants. The second is the CM reference frame of the dissociating molecule itself. According to the two-body model for CID the collisionally activated ion is scattered at some angle with internal energy defined by its shift with respect to the ESC. It then dissociates with random orientation between the dissociation axis and the momentum vector of the energized parent ion. The mass ratio effect in the second transformation results in significant broadening of the product ion velocity distribution. Finally, the fact that the average energy deposition remains nearly the same as collision energy increases suggests that the kinetic energy release in dissociation is also approximately constant.

The PEPICO experiments of Baer and co-worker [8] showed that the kinetic energy release for NO^+ from methyl nitrite ion with 0.8 eV internal energy is 0.054 eV. If we assume that average kinetic energy release in our CID experiments is also 0.054 eV (plausible as a zeroth order approximation since the average internal energy of the activated methyl nitrite ions after collision is of the same order and independent of collision energy), this kinetic energy release contributes to peak broadening of approximately 3.3, 3.3, and 4.6 eV for CID at 3.1, 19.8, and 39.8 eV collision energies, respectively. The kinetic energy distributions of the primary ion beam and the neutral beam also contribute to the observed peak width but are relatively small.

4. Discussion

The two-body treatment of CID of polyatomic cations intrinsically assumes that the internally excited ions decompose unimolecularly following the collisional activation step. The customary methodology for describing this step is the quasi-equilibrium theory/RRKM (QET/RRKM) model [24,25] described in detail in many places [26,27]. The most recent RRKM calculation for the methyl nitrite cation was published by Schroder et al. [13], who were primarily interested in the formation of the methoxy ion and its CH_2OH^+ isomeric structure. We present in Fig. 8 a plot of the rate coefficient for forming this ion. As noted earlier, this ion was observed in high intensity as a metastable ion but only in very low intensity as a CID product. To understand this observation and to aid our interpretation of our dynamics study of NO^+ formation we have calculated the rate of NO^+ formation.

According to the RRKM formalism the rate coefficient for formation of a given product ion is given by the expression

$$k(E^*) = L^{\ddagger}\frac{Q_1^+}{Q_1}\frac{\sum_{E_{vr}^+=0}^{E^+} P(E_{vr}^+)}{h\rho\,(E^*)} \qquad (2)$$

where $L^{\ddagger}$ is the reaction path degeneracy, h is Planck's constant, $\Sigma\, P\,(E_{vr}^+)$ is the sum of the number of vibrational–rotational quantum states of the transi-

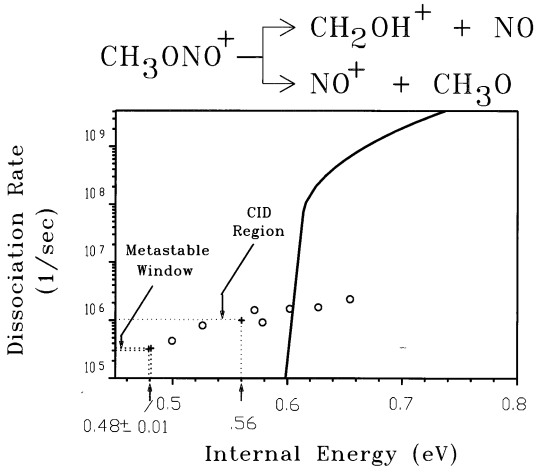

Fig. 8. Plot of dissociation rates for NO^+ (calculated from RRKM theory) and CH_2OH^+ (taken from Ref. [13]) as a function of internal energy. The horizontal dashed lines marked metastable window correspond to the dissociation limit observable within the field-free collision region in our instrument.

tion state with energies $\leq E^+_{vr}$, $\rho(E^*)$ is the density of states of the reactant ion with energy between E^* and $E^* + dE^*$, and Q^+_1 and Q_1 are the partition functions for the adiabatic rotations in the transition state and the ion, respectively. Table 1 summarizes the parameters which we used in our calculation of the rate of NO^+ formation. The vibrational frequencies were taken from Baer and Hass [8]. Our results are shown in Fig. 8.

The RRKM-based rate calculations provide important information for interpreting our CID dynamics study. Included in Fig. 8 are horizontal lines that are calculated boundaries for the rates of unimolecular dissociation that are detected in our experiments as metastable and CID products. Because ions arrive at the collision center of the our crossed-beam apparatus ~30 μs after they are formed by electron impact and have a transit time in the field-free collision zone of about 1 μs, the metastable "window" selects ions decaying with rates between 3.2×10^5 and 3.3×10^5 s^{-1}. This corresponds to a narrow range of internal energies for methyl nitrite ions of 0.48 ± 0.01 eV. Electron impact generates a readily detected population of ions with this amount of internal energy.

The Fig. 8 rate coefficient curves demonstrate why CH_2OH^+ is observed as a metastable ion whose CID intensity was too low for us to determine its dynamics and why NO^+ is the observable CID product. The rate curve for NO^+ formation becomes competitive at its threshold energy of 0.6 eV, where its unimolecular decay rate rises sharply from zero to a value greater than 10^6 s^{-1}. This fast direct dissociation reaction overpowers the reaction forming CH_2OH^+ at energies above 0.6 eV, effectively limiting the energy range where the rearrangement reaction product can be observed as a CID reaction product to the narrow internal energy window of observation to 0.56 ± 0.04 eV, effectively precluding any quantitative study of this reaction. It is therefore not surprising that, although we were able to detect m/z 31 as a CID product channel, we were unable to resolve it from the overlapping metastable ion decay process.

The horizontal line drawn at a rate coefficient of 1×10^6 s^{-1} marks the minimum rate for collisional activation of methyl nitrite cations which causes them to dissociate within the field free collision region prior to entering the linear-field lens for further analysis. The corresponding internal energy is about 0.6 eV.

Table 1
Parameters for the dissociation of methyl nitrite cation to NO^+; threshold energy: 13.8 kcal/mol, reaction path degeneracy: 1, temperature: 1000 K, internal rotor: CH_3

	Reactant ion	Transition state
Vibrational frequencies[a] (cm^{-1})	3600 (2), 2950, 1360 (3), 1110 (3), 900, 400, 300, 180, 160	3600 (2), 2950, 1360 (2), 1110 (3), 675, 400, 300, 180, 160
Symmetry factor	3	3
Moment of inertia (amu^2)	30.2, 365.2, 283.8	4.6, 469.2, 465.5
Reduced moment of inertia (amu^2)	2.8	2.72

[a] Taken from [8].

Combining this information with the internal energy content deduced from the observation of metastable decay to CH_2OH^+, which determines the maximum internal energy of the methyl nitrite cations to be about 0.5 eV with an average energy of 0.25 eV and leads to the qualitative prediction that the average energy converted from translational to internal energy in CID is of the order of 0.45 ± 0.25 eV. This prediction of average energy conversion following RRKM-based analysis supports our experimental results shown in Figs. 2–7.

The width of P(T) diagram at 3.1 eV collision energy is 2.7 eV FWHM, in reasonably good agreement with 3.3 eV predicted by the kinetic energy release data taken from PEPICO experiments. As previously noted, peak broadening increases dramatically with collision energy and the major factor is recoil kinetic energy in the fragments. This factor must be appropriately combined with the energy deposition function, both of which may depend on CM collision energy. As discussed by Futrell and co-workers [19,20,22] the energy deposition function for a single CID channel can be estimated by multiplication of the breakdown curve for this channel with the collisional energy deposition function. The internal energy present in the ion prior to collisional activation must also be added to this distribution. The energy deposition function for ions whose decomposition follows the RRKM theory has been shown to be adequately described in many cases by the Massey criterion [28]. The probability of depositing ΔE in a collision is given in its simplest form by the expression

$$P(\Delta E) \propto \exp(-a|\Delta E - \Delta E_0|/hv) \quad (3)$$

where ΔE_0 is the most probable energy transferred. The Massey hypothesis is that energy transfer is maximized when the energy transfer time $\Delta E/h$ matches the interaction time of the collision, a/v. The parameter a is called the "adiabatic parameter" which is of the order of atomic dimension (a few angstroms) and v is relative velocity.

For purposes of estimating the energy deposition function for CID of the methyl nitrite cation we chose

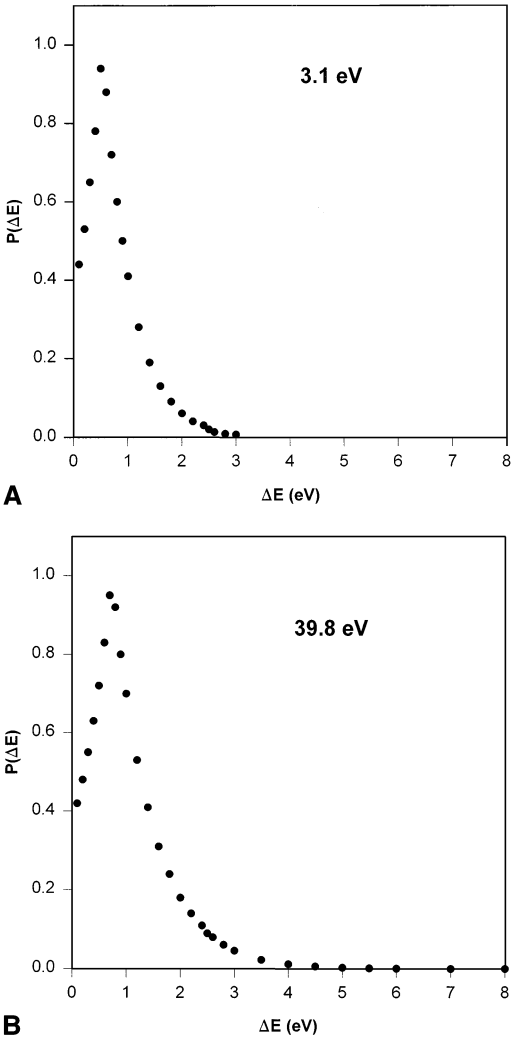

Fig. 9. Probability of energy transfer into the methyl nitrite cation calculated from the Massey's adiabatic criterion assuming the adiabatic parameter of 1 and (a) 3.1 eV, (b) 39.8 eV collision energies.

a equal to 1 Å and calculated most probable energy deposition, ΔE_0, using the relationship $a/v = \Delta E_0/h$ for each collision energy. In Fig. 9 the maximum energy allowed by energy and momentum conservation considerations is the CM collision energy. However, the exponential dependence of Eq. (3) restricts the probability to much lower values, as is observed experimentally for many systems including the methyl nitrite cation.

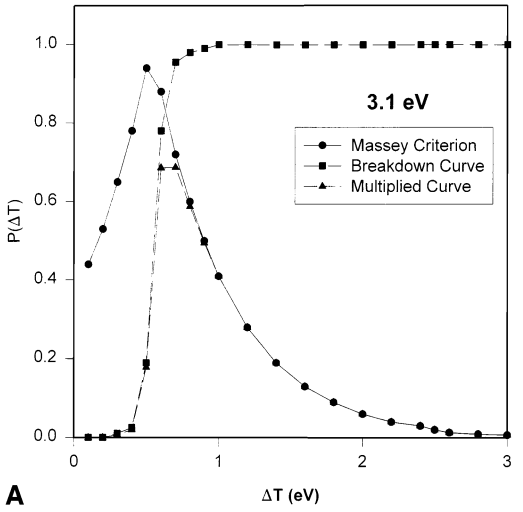

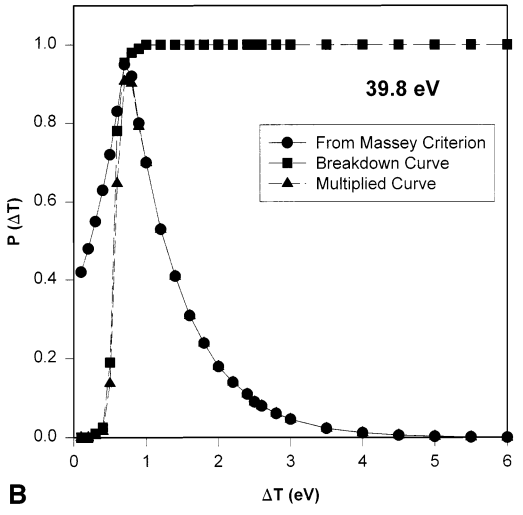

Fig. 10. Convoluted curves for the energy transfer probability from the PEPICO breakdown curve for NO^+ and the Massey's adiabatic criterion. (a) 3.1 eV, (b) 39.8 eV collision energy.

The Fig. 9 energy deposition functions are multiplied by the breakdown curve for NO^+ product ion taken from PEPICO experiments to obtain the predicted energy deposition curves for NO^+ formation in CID. Fig. 10(a) is such a curve for 3.1 eV collision energy and Fig. 10(b) for 39.8 eV collision energy. Consistent with our experimental observations, the most probable energy deposition increases only slowly with ion kinetic energy, from 0.5 eV at 3.1 eV collision energy to 0.7 eV at 39.8 eV. However the

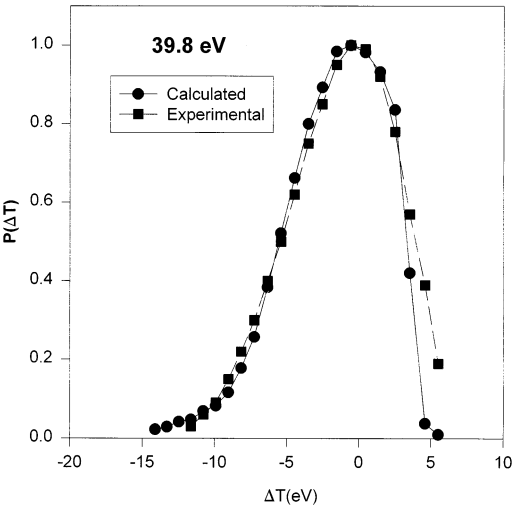

Fig. 11. Comparison of experimental P(T) diagram for 39.8 eV CID with the theoretical distribution obtained by convoluting the Fig. 10 probability curve with the ion beam profile due to 0.054 eV kinetic energy release in the dissociation step. An asymmetric Gaussian distribution with equivalent FWHM makes the best fit to our experimental distribution.

width of the distribution does change significantly, particularly at higher collision energy.

Fig. 11 shows the results of combining the Fig. 10(b) energy deposition function for NO^+ formation with kinetic energy release in the dissociation step (assumed equal to 0.054 eV, as discussed previously) and with the energy spread of the primary ion beam. Comparison of Fig. 11 with Fig. 7 replotted and normalized in Fig. 11, satisfactorily accounts for both the observed broad energy distribution of product ions and the scattering of a moderate intensity of product ions outside the ESC. Although not unique, the plausible Massey criterion parameters provide a remarkably good fit to our experimental observations. We conclude that this description satisfactorily rationalizes our results at all three collision energies.

We conclude our discussion of CID of the methyl nitrite cation by recalling our previous study of the dynamics of the isomeric nitromethane cation which demonstrated that NO^+ is formed in this system with relatively small energy conversion and is forward scattered over the same collision energy as the present study. We proposed that isomerization from the ni-

tromethane structure to the methyl nitrite ion precedes the dissociation step in low energy CID of nitromethane cations. Referring to Fig. 1, the present experiments follow the dissociation path beginning with vibrationally excited methyl nitrite ions containing an average of 0.2 eV internal energy and must overcome a barrier height of 0.6 eV to dissociate. Nitromethane ions are in a deeper potential well, contain up to 0.5 eV internal energy, and have a 0.7 eV barrier to surmount. The rearrangement to methyl nitrite ion is the slow step in the dissociation mechanism; once it occurs, dissociation proceeds on the same potential surface as the present reaction.

Compared with the forward-scattered peak for the same NO^+ ion from CID of nitromethane ion, the CID peak of methyl nitrite ion shows slightly higher energy transfer and larger scattering angle. This behavior is expected since the dissociation from this lower point in the potential energy surface requires deposition of more energy to proceed rapidly; further, the internal energy of the molecular ion is smaller than in nitromethane ion. Once the internal energy of methyl nitrite ion exceeds 0.6 eV, it dissociates rapidly with rates exceeding 7×10^6 s^{-1}.

5. Conclusions

The dissociation of the methyl nitrite cation into NO^+ and methoxy radical occurs via an impulsive mechanism over the investigated collision energy range of 3–40 eV. The average kinetic energy converted into internal energy to drive the reaction is close to the thermochemical threshold for the process and changes only modestly with collision energy. It ranges from 0.5 eV at the lowest collision energy to 0.7 eV at the highest with an experimental uncertainty of the order of 0.5 eV. The width of the distribution is quite broad and increases with collision energy. Substantial intensity is found outside the elastic scattering circle, mainly in the forward scattering direction. The major factor contributing to the broad distribution observed is kinetic energy release in the dissociation step.

Our results are rationalized in terms of a single mechanism in which ground state ions are collisionally activated and dissociate over the lowest energy barrier via direct rupture of the CH_3O–NO bond. The experimental results just summarized are quantitatively explained by combining RRKM modeling of the dissociation process with an energy distribution function based on Massey's adiabatic hypothesis and kinetic energy release measured from PEPICO experiments. An upper limit to internal energy present in the methyl nitrite cation when it is formed by electron impact of 0.48 ± 0.04 eV is also established by the analysis.

Combining this information with previous results from our laboratory on the dynamics of the CID of nitromethane cation strongly supports the mechanism which we proposed for this ion. Specifically, it supports the suggestion that the low energy dissociation channel involves the isomerization of the nitromethane cation into the methyl nitrite structure, which immediately dissociates via the mechanism deduced in the present research. The higher collision energy channel in nitromethane cation CID proceeds via a nonadiabatic transition to an upper electronic hypersurface from which the dissociation occurs. There is no evidence from the present study that non-adiabatic pathways are followed in the dissociation of methyl nitrite cation.

Acknowledgements

The support of this research by NSF grant nos. CHE-9021014 and CHE-9616711 is gratefully acknowledged.

References

[1] S. Meyerson, E.K. Field, Org. Mass Spectrom. 9 (1974) 485.
[2] Y. Niwa, S. Tajima, T. Tsuchiya, Int. J. Mass Spectrom. Ion Phys. 40 (1981) 287.
[3] J.P. Gilman, T. Hsieh, G.G. Meisels, J. Chem. Phys. 78 (1983) 1174.
[4] C. Lifshitz, M. Rejwan, I. Levin, T. Peres, Int. J. Mass. Spectrom. Ion Processes 84 (1987) 271.
[5] H. Egsgaard, L. Carlsen, Ber. Bunsenges. Phys. Chem. 90 (1986) 369.

[6] I.K. Ogden, N. Shaw, C.J. Danby, I. Powis, Int. J. Mass Spectrom. Ion Processes 54 (1983) 41.
[7] J.P. Gilman, T. Hsieh, G.G. Meisels, J. Chem. Phys. 78 (1983) 3767.
[8] T. Baer, J.R. Hass, J. Phys. Chem. 90 (1986) 451.
[9] J.C. Lorquet, C. Barbier, B. Leyh-Nihant, Adv. Mass Spectrom. 10 (1986) 71.
[10] E.E. Ferguson, Chem. Phys. Lett. 138 (1987) 450.
[11] M.P. Irion, A. Selinger, A.W. Castleman, Jr., E.E. Ferguson, K.G. Weil, Chem. Phys. Lett. 147 (1988) 33.
[12] G.G. Meisels, T. Hsieh, J.P. Gilman, J. Chem. Phys. 73 (1980) 4126.
[13] D. Schroder, D. Sulzle, O. Dutuit, T. Baer, H. Schwarz, J. Am. Chem. Soc. 116 (1994) 6395.
[14] P.C. Burgers, J.L. Holmes, Org. Mass Spectrom. 19 (1984) 452.
[15] B. Leyh-Nihant, J.C. Lorquet, J. Chem. Phys. 88 (1988) 5606.
[16] E.W.R. Steacie, D.S. Calder, J. Chem. Phys. 4 (1936) 96.
[17] A.H. Blatt (Ed.), Organic Synthesis, Wiley, New York, 1963, Vol. 2, p. 363.
[18] A.K. Shukla, S.G. Anderson, S.L. Howard, K.W. Sohlberg, J.H. Futrell, Int. J. Mass Spectrom. Ion Processes 86 (1988) 61.
[19] A.K. Shukla, J.H. Futrell, Mass Spectrom. Rev. 12 (1993) 211.
[20] A.K. Shukla, J.H. Futrell, in Experimental Mass Spectrometry, D.H. Russell (Ed.), Plenum, New York, 1994.
[21] I.W.M. Smith, Kinetic and Dynamics of Elementary Gas Reaction, Butterworths, London, 1980.
[22] A.K. Shukla, K. Qian, S.G. Anderson, J.H. Futrell, Int. J. Mass Spectrom. Ion Processes 109 (1991) 227.
[23] B. Friedrich, Z. Herman, Collect. Czech. Chem. Comm. 49 (1984) 570.
[24] R.A. Marcus, O.K. Rice, J. Phys. Colloid Chem. 55 (1951) 894.
[25] H.M. Rosenstock, M.B. Wallenstein, A.L. Wahrhaftig, H. Eyring, Proc. Natl. Acad. Sci. USA 38 (1952) 667.
[26] K.A. Holbrook, M.J. Pilling, S.H. Robertson, Unimolecular Reactions, Wiley, New York, 1996.
[27] T. Baer, W.L. Hase, Unimolecular Reaction Dynamics, Oxford University Press, Oxford, 1996.
[28] H.S.W. Massey, Rep. Prog. Phys. 12 (1949) 249.